Exp Oncol 2011
33, 3, 130–135

Experimental ONCOLOGY

NANOHYPERTHERMIA OF MALIGNANT TUMORS. I. LANTHANUM-STRONTIUM MANGANITE MAGNETIC FLUID AS POTENTIAL INDUCER OF TUMOR HYPERTHERMIA

S. Solopan[1,], A. Belous[1], A. Yelenich[1], L. Bubnovskaya[2], A. Kovelskaya[2], A. Podoltsev[3], I. Kondratenko[3], S. Osinsky[2]*

[1]*V.I. Vernadsky Insitute of General and Inorganic Chemistry, NAS of Ukraine, Palladin Ave. 32/34, 03680 Kiev, Ukraine;*

[2]*R.E. Kavetsky Institute of Experimental Pathology, Oncology and Radiobiology, NAS of Ukraine, Vasilkovskaya Str. 45, 03022, Kiev, Ukraine*

[3]*Institute of Electrodynamics, NAS of Ukraine, Peremoga Ave. 56, 03057, Kiev, Ukraine*

***Objectives*: To synthesize magnetic particles of lanthanum-strontium manganite, prepare the magnetic fluid (MF), evaluate the generation of heat by particles and determine their common toxicity. *Methods*: Nanoparticles based on the solid solutions of lanthanum-strontium manganite ($La_{1-x}Sr_xMnO_3$) have been synthesized by a sol-gel method. Conventional methods of experimental oncology were used. *Results*: Nanoparticles of ferromagnetic materials on the basis of solid solutions of lanthanum strontium manganite by sol-gel method were synthesized. It was shown the possibility to regulate the aggregate form of particles that are formed during the synthesis. Magnetic fluid based on the synthesized nanoparticles and water solutions of agarose have been produced. It was shown the possibility to heat this magnetic fluid up to 42–45 °C in externally applied alternating magnetic field (AMF) operated at 100–400 kHz. It was determined that under long-term influence of AMF nanofluid is heated up to temperature which is not over that of magnetic phase transition. It was detected that magnetic powder as well as fluid have not displayed acute toxicity or side effects (intraperitoneal or intratumoral administration) in animals either intact or with transplanted tumors. *Conclusions*: Possibility of synthesized magnetic fluid to generate heat in externally applied AMF as well as lack of side effects allow to consider its as a potential mean for tumor hyperthermia (HT).**

***Key Words*: ferromagnetic materials, sol-gel synthesis, hyperthermia, magnetic fluid, nanosized particles.**

Hyperthermia (HT) is applied in combination with radiation and/or chemotherapy in the treatment of patients with severe malignant tumors more than 30 years demonstrating significantly enhancement of therapy outcome [1–5]. At the same time, some of the basic problems of HT, in particular receiving the homogeneous distribution of temperature in tumor volume and heating the deep-seated tumors are not resolved till now despite of intensive efforts in the field of technical arrangement of clinical HT.

Among the different approaches to overcome above mentioned problems and enhance the HT efficacy the nanotechnology seems to be the most promising. At the present time the studies dedicated to the synthesis of magnetic nanoparticles for the biomedical applications are became the more and more intensive. Organic and inorganic nanoparticles are widely used in the diagnostics and treatment of various diseases, in particular neoplastic one [6–8]. Special interest is focused on the ferromagnetic nanoparticles that can be heated by externally applied alternating magnetic field resulting in the heating of tumor tissue [9–11]. It was shown that the application of magnetic nanoparticles in the combined cancer treatment allows to enhance the therapy efficacy [12–17].

Up to date, the most common magnetic materials for tumor hyperthermia as well as for drug delivery are magnetite (Fe_3O_4) and maghemite (γ-Fe_2O_3) the biocompatibility of which are well known [11, 18, 19].

It has to be mentioned that the highest achievements in the field of nanohyperthermia were received by Jordan et al. [13, 15, 16]. They have elaborated the method of local heating of tumor by means of magnetic fluid (Fe_3O_4 particles with 15–20 nm in size) that was injected into the tumor followed by exposition of tumor to an alternating magnetic field (100 kHz frequency) that resulted in the increase of tumor temperature up to 44–45 °C. The coating of nanoparticles by aminosylane forms the preventive "sleeve" around the core of iron oxide that helps to particles to be absorbed by tumor cells in more significant amount and to avoid the withdrawal from tumor [11, 17].

It has to be noted that one problem is discussed now very actively, namely the possible negative influence of ferromagnetic materials with high Curie temperature on hyperthermic procedure, in particular excessive heating of surrounding healthy tissues and other side effects by the exploitation of the following nanoparticles: Fe_3O_4 (585 °C), γ-Fe_2O_3 (447 °C), $CoFe_2O_4$ (518 °C), $ZnFe_2O_4$ (545 °C) and $BaFe_{12}O_{19}$ (580 °C) [20, 21].

Nanoparticles with the phase transition in the temperature range 42–45 °C that are optimal for the destruction of malignant tumors, may be exploited as safety alternative for tumor HT. The heterosubsitute lanthanum-strontium manganites were considered as a very promising to achieve this aim: $La_{1-x}A_xMnO_3$ (where A = Ag, Ba, Ca, Na, Sr) [22–25].

Received: July 26, 2011.

*Correspondence: E-mail – solopan@ukr.net

Abbreviations: AMF – alternating magnetic field; HT – hyperthermia.

These substances demonstrate the ferromagnetic effect in the range of x=0.25–0.5 with Curie point = 0–95 °C.

On the current days there is a large number of methods for nanosized ferromagnetic materials preparation. One of the promising methods is a sol-gel method, the use of which can produce crystal nanoparticles and decrease the temperature of the single-phase product synthesis.

Moreover, there is very important to create on the basis of ferromagnetic nanoparticles the magnetic fluids (MF) which could be heated by the exposition to AMF and characterized by high level of biocompatibility.

The current study was aimed to synthesize magnetic particles of lanthanum-strontium manganite, evaluate structural and electrical properties of nanosized particles, create the ferromagnetic fluid, determine their heating by AMF, and assess of MF toxicity *in vivo*.

MATERIALS AND METHODS

Synthesis of nanoparticles. Samples of the solid solution $La_{1-x}Sr_xMnO_3$ (x_{Sr} = 0.225–0.3), have been synthesized by the sol-gel method [26, 27]. Water-soluble salts $La(NO_3)_3$, $Sr(NO_3)_2$, $Mn(NO_3)_2$ were used as starting reagents. Calculated amounts of reagents were dissolved in distilled water. Citric acid and ethylene glycol as gelling additives were added to the solution. When the mixture is heated at 80 °C, polyesterification occurs with the formation of polymeric gel. Then the temperature increased up to 200 °C, and powder of $La_{1-x}Sr_xMnO_3$ precursor was formed as a result of pyrolysis. Heat treatment of obtained powders of "precursor" was performed in the temperature range 400–1100 °C in a crucible from Al_2O_3 in the air for 2–4 h. For comparison, the control samples have been also synthesized by the method of solid state reactions and by precipitation from solution. Synthesis of samples by solid-state reactions were carried out as described in [28]. Synthesis of the samples by precipitation from solution was carried out as described in [29].

Physic-technical methods. X-ray diffraction (XRD) measurements were carried out on a "DRON-4–07" diffractometer (Cu*K*α radiation) in the range of 2θ = 10–150 °C.

Alternating magnetic field. A high frequency generator produced by Institute of Electrodynamics was used to induce an alternating current of 70 A at a frequency of 100–440 kHz. The equipment is shown in Fig. 1. The current passes through a custom-made five-turn water-cooled coil of 30 mm in internal diameter and 30 mm in height to generate a magnetic field inside the coil. The electromagnetic field within this coil is not uniform. The sample with magnetic fluid was placed on a platform in a center inside the coil with maximum magnetic field strength above 7.7 kA/m (Fig. 2, *a*, 2, *b*, and 2, *c*). According to the heating mechanisms of nanoparticle hyperthermia, the induced energy generation rate is approximately proportional to H^2. But a characteristic size of the sample was relatively small (8 mm in diameter and 15 mm in height), and a variation of the magnetic field inside the whole sample can be considered negligible.

Fig. 1. Experimental setup consisting of a high frequency generator (*a*) and coil (*b*)

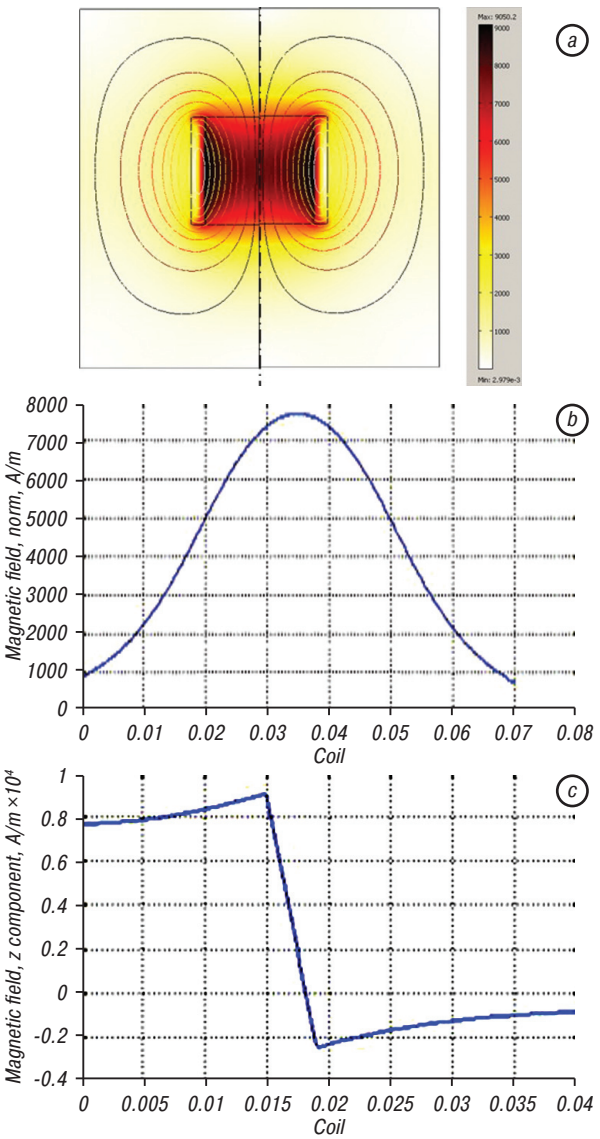

Fig. 2. Distribution of magnetic field |H| in the coil (*a*) and magnetic field H_z on the vertical (*b*) and horizontal (*c*) axis of symmetry

Temperature measurement. The temperature monitored by fine thermocouple (copper-constantan) were recorded every 60 s during the entire experiment. At this moment the high frequency generator was turn off at a small interval of time ~5 s.

Biological studies. In accordance with the methodological instructions the normal animals have been used in this study. The experiments were conducted with intact C57Bl/6 mice (bred of Institute of Experimental Pathology, Oncology and Radiobiology), males with body weight of 20–22 g. There were 6 animals in each experimental group. It was used 30 normal mice to determine the acute toxicity, 8 Lewis lung carcinoma-bearing mice (C57Bl/6, male, 20–22 g, intramuscular transplantation) and 15 Guerin carcinoma-bearing rats (IEPOR bred, female, 170–200 g, subcutaneous translpantation). All experiments had been approved by the regional animal ethics committee.

RESULTS AND DISCUSSION

According to the method of sol-gel synthesis, the addition of gel-forming substances to the salts of metals and subsequent heating results in the series of processes in solution, in particular the formation of heteronuclear metal complexes with citric acid as well as citric acid polymerization with ethylene glycol described in the literature [27, 30, 31]. The polymerization of the gel was carried out at different pH. The solution of ammonia was added into obtained gel to change pH with the following evaporation of solutions to obtain a powder "precursor". The powders obtained at different pH and temperatures of heat-treatment were investigated by X-ray and electron microscopy (Fig. 3 and 4).

As shown in Fig. 3, *a*, the broad halo in the field of 2θ = 20–25° is observed for the powder "precursor" synthesized in acidic environment (pH = 1.5) at 400 °C, that indicates its amorphous state. Further heat-treatment leads to the crystallization of the sample that was initiated in the temperature range of 500–600 °C. After heat treatment at 800 °C the sample is a single phased according to X-ray analysis, but a slight broadening of the main peaks were observed on X-ray slides. At the same time, according to electron microscopic studies (Fig. 4, *a*), the investigated particles have amorphous and crystalline regions, that is also confirmed by electron diffraction analysis. After analyzing the results of electron diffraction of amorphous particles as well as X-ray data it was concluded that the amorphous regions, which are observed in the agglomerates are carbon that is not oxidized during the pyrolysis of gel. Detailed microstructural analysis of crystalline particles showed that their sizes are within 20–50 nm. The particles form dense agglomerates with size ranged 500–2000 nm.

According to X-ray analysis for samples obtained at a pH of the gel, equal to 6 (Fig. 3, *b*), after heat treatment at 400 °C there is a somewhat different picture, namely, the samples are partially amorphous and partially crystalline, as evidenced by an amorphous halo in the field of 2θ = 20–25 °C, as well as the presence of broad peaks, indicating the beginning of the formation of crystalline compounds.

The micrographs and electron diffraction data for solid solution $La_{0.775}Sr_{0,225}MnO_3$, synthesized at pH = 6 after heat treatment at 800 °C were presented on Fig. 4, *b*. For this sample, the formation of agglomerates consisting from smaller units, occurs which, in turn, are formed from the nanoparticles. These agglomerates are formed by the crystal particles and have not the amorphous phase, unlike the previous model. As seen from the microphotograhs, the size of the particles that form the agglomerates is 50–70 nm.

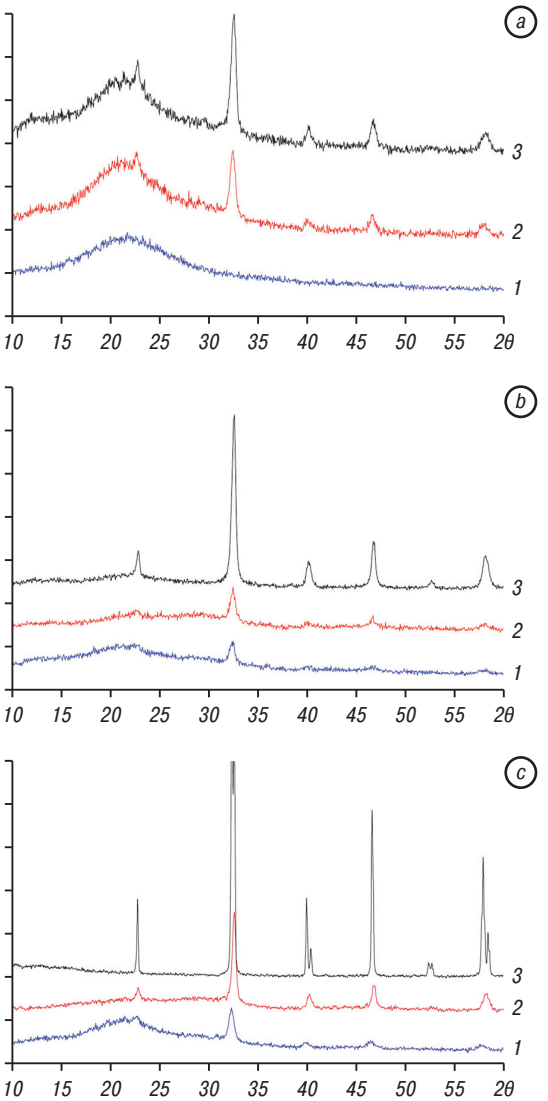

Fig. 3. X-ray patterns of precursor for receiving of solid solution $La_{0.775}Sr_{0,225}MnO_3$ after thermotreatment at different temperature: 400 °C (1); 600 °C (2); 800 °C (3). Gel pH ~ 1.5 (***a***), 6 (***b***), 9 (***c***)

The X-ray powder diffraction patterns of samples obtained at gel pH=9 (Fig. 3, *c*) after heat treatment contain only crystalline particles. X-ray peaks are narrow, indicating a high degree of sample crystallinity. For a solid solution $La_{0.775}Sr_{0,225}MnO_3$, synthesized at pH = 9, after heat treatment at 800 °C, the formation of "soft" slightly-agglomerated powders with a loose structure of the agglomerates, in which the particles have a size of about 40–50 nm (Fig. 4, *c*) was observed. In this case, as seen from the figure, the particles are fully crystal.

In accordance with Brinker and Scherer, and Kabihana [31, 32], observed pH influence is associated with

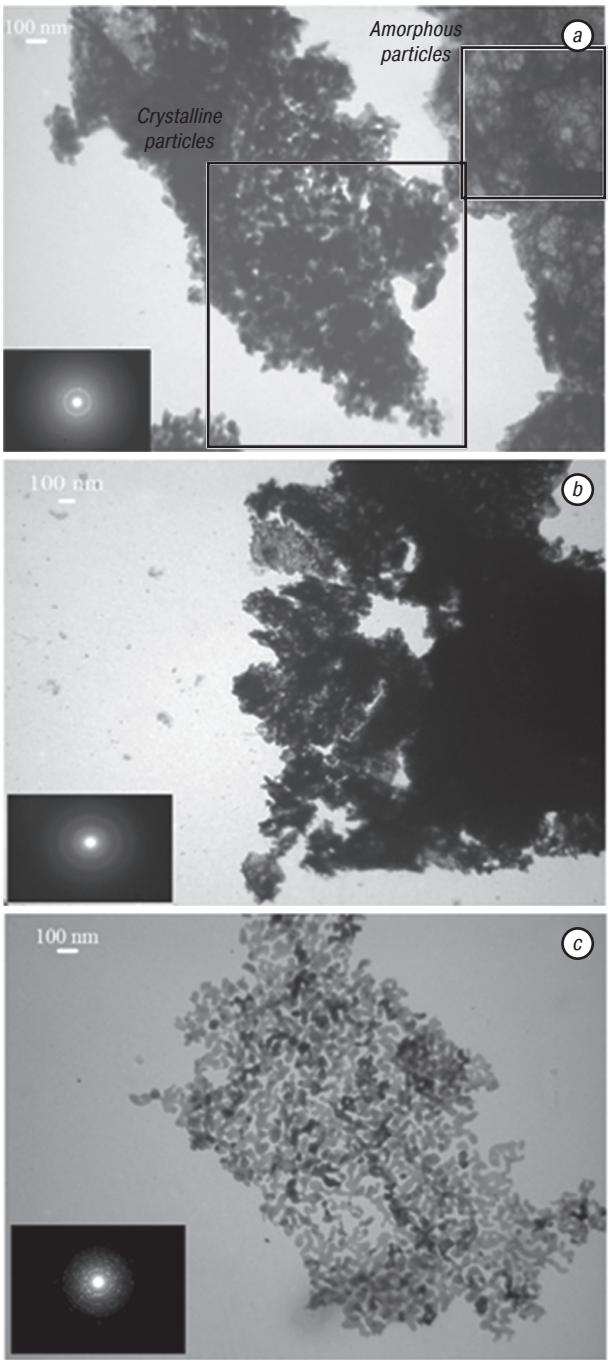

Fig. 4. Microphotographs of particles of solid solution $La_{0.775}Sr0{,}0225MnO_3$ synthesized at 800 °C during 2 h. Gel pH ~ 1,5 (*a*), 6 (*b*), 9(*c*)

the fact that the formation of metal complexes with citric acid and their subsequent polymerization with ethylene glycol under acidic environment (pH=1.5) was occurred. Under alkaline environment (pH=9), the formation of hydroxides of metals and their interaction with the polymer gel is caused by the formation of hydrogen bonds.

It should be noted that the formation of single-phased crystal structure by using the method of solid state reactions occurs in the temperature range 1000–1150 °C while the precipitation from solutions the single-phase crystalline structure is formed at 1350 °C, which is consistent with Belous et al. [29].

Our studies have shown that using the proposed method of sol-gel synthesis of solid solutions of the system $La_{0.775}Sr_{0.225}MnO_3$ the single-phased crystal structure begins to be formed at 500–600 °C, and at 800 °C the samples are fully crystal (Table). The particle size is about 40–50 nm. On the basis of synthesized nanoparticles $La_{0.775}Sr_{0.225}MnO_3$ the magnetic fluid was obtained where the aqueous solutions of agarose as gel-forming component was used.

The results of investigations of "agarose" aqueous solution viscosity and the maximum permissible viscosity of fluids in living organisms have shown in Fig. 5 [33]. It was concluded that the optimum concentration of base material (agarose) should not exceed 0.06%. The magnetic particles of a solid solution of $La_{0.775}Sr_{0.225}MnO_3$, synthesized both by solid state reaction method and sol-gel method with different temperatures of heat-treatment (T_{term} = 800, 900, 1000, 1100, 1150°C) were used to evaluate the influence of magnetic properties of the substance on magnetic fluid heating.

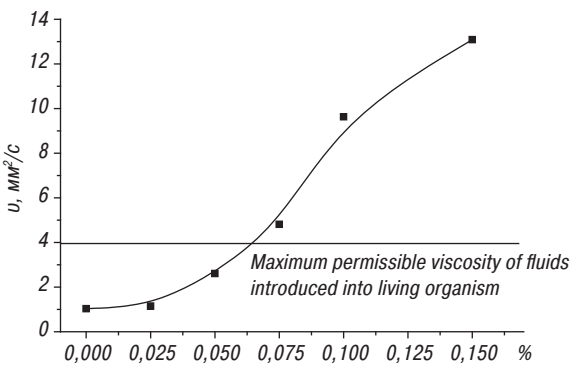

Fig. 5. Dependence of gel viscosity prepared by means of agarose on the basic substance concentration

Table. Phase composition of manganites $La_{0.775}Sr_{0.225}MnO_3$ powders according to conditions of synthesis and thermotreatment temperature*

T, K	Solid phase synthesis	Synthesis by precipitation from solutions	Sol-gel synthesis
870	Mn_2O_3(100), La_2O_3(78), $SrCO_3$(57), $La(OH)_3$(32),** SrO(32), P(8), $SrMnO_3$(8)	P(100), $La_2O_2CO_3$(44), Sr_2MnO_5(32), Sr_2MnO_4(16), Mn_2O_3(14), $SrCO_3$(3)	P(100)
970	Mn_2O_3(100), La_2O_3(78), $SrCO_3$(57), $La(OH)_3$(32),** SrO(32), P(8), $SrMnO_3$(8)	P(100), $La_2O_2CO_3$(44), Sr_2MnO_5(32), Sr_2MnO_4(16), Mn_2O_3(14), $SrCO_3$(3)	P(100)
1070	La_2O_3(100), Mn_2O_3(97), P(72), a-$SrMnO_3$(13)	P(100), $Sr_2Mn_2O_5$(12), $La(OH)_3$(11), Mn_2O_3(9), $(La_1\text{-}ySry)_2MnO_4$(7), $La_2O_2CO_3$(5)	P(100)
1170	P(100), Mn_2O_3(33), $La(OH)_3$(14), a-$SrMnO_3$(5), $SrCO_3$(3), SrO(3)	P(100), $Sr_2Mn_2O_5$(7), $La(OH)_3$(4), $(La_1\text{-}ySry)_2MnO_4$(4), $La_2O_2CO_3$(1)	P(100)
1270	P(100), La_2O_3(11), a-$SrMnO_3$(3), Mn_3O_4(1.5)	P(100), $Sr_2Mn_2O_5$(4), $(La_1\text{-}ySry)_2MnO_4$(2), $La_2O_2CO_3$(0.7)	P(100)
1320	P(100), La_2O_3 (**traces**)	–	P(100)
1370	P(100)	P(100), $Sr_2Mn_2O_5$(4), $(La_1\text{-}ySry)_2MnO_4$(1.7), $La_2O_2CO_3$(0.6)	P(100)
1570	P(100)	P(100), $(La_1\text{-}ySry)_2MnO_4$(1), $La_2O_2CO_3$(**traces**)	P(100)
1620	P(100)	P(100)	P(100)

*Numbers in parentheses – relative intensity of most reflexes in corresponding phases (%);

**Appearance of $La(OH)_3$ is caused by La_2O_3 absorption of water from air under storage; P – perovskite.

AMF resting. The heating of magnetic fluids were carried out in an alternating magnetic field in the frequency range of 100–400 kHz. It was determined that the heating of magnetic fluids of all prepared samples to a constant temperature was observed during 20 minutes (Fig. 6). It was also shown that the temperature of the synthesis of magnetic particles impact on the heating temperature of magnetic fluids. This regularity can be explained by changes in the ratio Mn^{3+}/Mn^{4+} [34–36], which results in the change of Curie temperature and conductivity as well as particle sizes [37]. The dependence of the magnetization of $La_{0.775}Sr_{0.225}MnO_3$, synthesized by sol-gel method at pH = 9, from the magnetic field parameters was evaluated. It was found that the coercitive force of this powder (Hc) is 2834.39 A/m, and the magnetization (Ms) is 4.79 Gc cm^3/g, whereas the theoretical Ms for its is 91.5 Gc cm^3/g.

Toxicity of magnetic fluid. It was determined the maximal tolerable dose (MTD) in accordance with instructions. Conventional indices of acute toxicity, such as LD_{10}, LD_{50}, LD_{100} could not been determined because of low toxicity of tested substance that resulted in the necessity to apply of overdoses of nanopowder. MTD was determined as a dose that does not results in the death of no one animal in the group and at the same time does not provoke body weight loss not more than 10%. The substance that results in the body weight loss more than 10% is considered toxic. In order to designate the toxicity of the substance each animal was weighed before it administration and every day after up to the end of experiment.

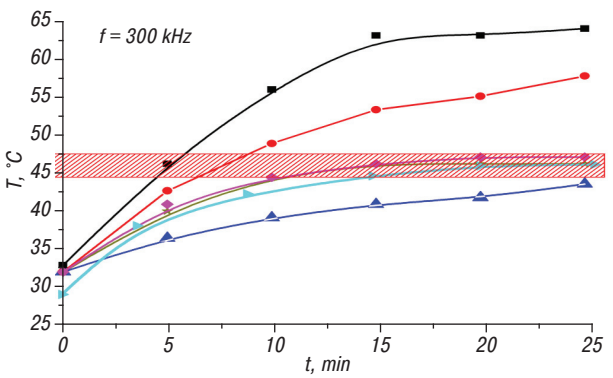

Fig. 6. Time-dependent heating of MF, based on agarose and $La_{0.775}Sr_{0.225}MnO_3$, induced with AMF (300 kHz, strength of 7.1 kA/m). 1, 2 — the samples were synthesized by the method of solid-phase reaction at 1200 and 1150 °C, respectively; 3, 4, 5, 6 — the samples were synthesized by sol-gel method at 900, 800, 1000 and 1100 °C, respectively. The shaded area indicates the optimal temperature for tumor hyperthermia

Magnetic fluid (sol-gel method, T_{term} = 800 °C) was administered into the mice at the doses of 100, 200, 300 and 400 mg of powder of nanoparticles/kg of body weight. It was given intraperitoneally, in a single dose. Duration of observation under every group was 14 days.

Under the administration of this substance at the doses of 50 and 100 mg/kg body weight loss was not observed on the 1st day after. On the contrary it was observed body weight increase gradually up to the end of experiment and approximately on 26±3.0% more that it was before substance administration.

Beginning from a dose of 200 mg/kg it was observed inconsequential body weight loss on the 1st day after injection — by 1.6±0.4% compare with the initial ones and than body weight loss increased with the increase of doses administered: at a dose of 300 mg/kg — by 7.5±1.5%, at a dose of 400 mg/kg — by 8.5±2.1%.

At a dose of 200 mg/kg as early as on the 4th day after injection it was observed that body weight was not only restored but it was going on gradual increasing by 25±2.1% up to the end of experiment.

At a dose of 300 mg/kg rather substantial body weight loss 7.5±1.5% was registered already on the 1st day after. On the 2nd and 3rd days animal body weight started to restore gradually but not substantial: by 2.45±0.9% and by 2.1±0.6%, respectively. Beginning from the 4th day after injection body weight of almost all mice returned to the initial level and then started to be increased by 6.8±0.5% and 9.1±1.8% on the 4th and 7th days, respectively.

Dose of 400 mg/kg of body weight caused the most substantial body weight loss by 8.5 ±2.3% on the 1st day after injection and continue to be observed on the 2nd, 3rd and 4th day: by 5.3±2.1%, 2.3 ±1.7% and 1.6 ±0.7%, respectively, in comparison with initial body weight of the mice. In further it was observed that body weight loss gradually started to delay and beginning from the 7th day mice body weight was increased by 3.3±1.1% and at the end of the experiment (at the 14th day) it was 5.6±2.8% higher.

On the grounds of the obtained results it was possible to make the conclusion that maximum tolerable dose (MTD) is 300 mg/kg of body weight.

In conclusion, the nanoparticles of a solid solution $La_{0.775}Sr_{0.225}MnO_3$ produced by sol-gel method was synthesized and magnetic fluid on their basis prepared. It was shown the possibility to control the size and aggregate state of particles by changing the synthesis conditions. The physical parameters of the synthesized nanoparticles were evaluated, and it was shown the change of the phase transition temperature from ferromagnetic to paramagnetic state for the synthesized nanoparticles. The possibility to heat the magnetic fluid obtained on the basis of mentioned nanoparticles up to 42–45 °C in an alternating magnetic field was demonstrated. It was also established that the temperature of heated fluid was not exceeded the temperature of magnetic phase transition under prolonged exposure to AMF.

It was determined that synthesized nanoparticles of lanthanum strontium manganite ($La_{0.775}Sr_{0.225}MnO_3$) did not display the toxicity or provoked the side effects being administered intraperitoneally into the experimental animals neither intact nor with transplanted tumors. Maximum tolerable dose (MTD) of nanopowder is 300 mg/kg of body weight.

ACKNOWLEDGEMENTS

This work was supported by STCU (grant #5213).

REFERENCES

1. **van der Zee J, Vujaskovich Z, Kondo M, Sugahara T.** The Kadota Fund International Forum 2004 — clinical group consensus. Int J Hyperthermia 2008; **24**: 111–22.

2. **Beasley GM, Ross MI, Tyler DS.** Future directions in regional treatment strategies for melanoma and sarcoma. Int J Hyperthermia 2008; **24**: 301–9.

3. **Schlemmer M, Wendtner CM, Lindner L, *et al.*** Thermochemotherapy in patients with extremity high-risk soft tissue sarcomas. Int J Hyperthermia 2010; **26**: 127–35.

4. **Zagar T, Oleson JR, Vujaskovich Z, *et al.*** Hyperthermia combined with radiation therapy for superficial breast cancer and chest wall recurrence: a review of the randomised data. Int J Hyperthermia 2010; **26**: 612–7.

5. **Zagar T, Oleson JR, Vujaskovich Z, *et al.*** Hyperthermia for locally advanced breast cancer. Int J Hyperthermia 2010; **26**: 618–24.

6. **Cho K, Wang X, Nie S, *et al.*** Therapeutic nanoparticles for drug delivery in cancer. Clin Cancer Res 2008; **14**: 1310–6.

7. **Lammers T, Hennink WE, Storm G.** Tumor-targeted nanomedicines: principles and practice. Br J Cancer 2008; **99**: 392–7.

8. **Scheinberg DA, Villa CH, Escorcia FE, *et al.*** Conscripts of the infinite armada: systemic cancer therapy using nanomaterials. Nat Rev Clin Oncol 2010; **7**: 266–76.

9. **Mornet S, Vasseur S, Grasset F, *et al.*** Nagnetic nanoaprticles design for medical diagnosis and therapy. J Mater Chem 2004; **14**: 2161–75.

10. **Gupta K, Gupta M.** Synthesis and surface emgineering of iron oxide nanoparticles for biomedical applciaitons. Biomater 2005; **26**: 3995–4021.

11. **Barry SE.** Challenges in the development of magnetic particles for therapeutic applications. Int J Hyperthermia 2008; **24**: 451–66.

12. **Thiesen B, Jordan A.** Clinical applications of magnetic nanoparticles for hyperthermia. Int J Hyperthermia 2008; **24**: 467–74.

13. **Jordan A.** Hyperthermia classic commentary: "Inductive heating of ferrimagnetic particles and magnetic fluids: Physical evaluation of their potential for hyperthermia" by Jordan A et al., Int J Hyperthermia 1993; **9**:51–68. Int J Hyperthermia 2009; **25**: 512–6.

14. **Krishnan S, Diagaradjane P, Cho SH.** Nanoparticles-mediated thermal therapy: evolving strategies for porstate cancer therapy. Int J Hyperthermia 2010; **26**: 775–89.

15. **Johannsen M, Thiesen B, Wust P, *et al.*** Magnetic nanoparticle hyperthermia for prostate cancer. Int J Hyperthermia 2010; **26**: 790–5.

16. **Maier-Hauff K, Rothe R, Scholz R, *et al.*** Intracranial thermotherapy using magnetic nanoparticles combined with external beam radiotherapy: results of a feasibility study on patients with glioblastoma multiforme. J Neurooncol 2011; **103**: 317–24.

17. **Silva AC, Oliveira TR, Mamani JB, *et al.*** Application of hyperthermia induced by superparamagnetic iron oxide nanoparticles in glioma tretament. Int J Nanomedicine 2011; **6**: 591–603.

18. **Klokkenburg M, Vonk Ch, Claesson M, *et al.*** Direct imaging of zero-field dipolar structures in colloidal dispersions of synthetic magnetite. J Am Chem Soc 2004; **126**: 16706–7.

19. **Hergt R, Hiergeist R, Hilger I, *et al.*** Review: magnetic nanoparticles for thermoablation. Rec Res Develop Mat Sci 2002; **3**: 723–42.

20. **Vasseur S, Dudeut E, Portier J, *et al.*** Lanthanum manganese perovslite nanoparticles as possible in vivo mediators for magnetic hyperthermia. J Magn Magn Mater 2006; **302**: 315–20.

21. **Pollert E, Knizek K, Mazusko M, *et al.*** Mew *T*c-tuned magnetic nanoparticles for self-controlled hyperthermia. J Magn Magn Mater 2007; **316**: 122–5.

22. **Pradhan AK, Mundic R, Rakhimov RR, *et al.*** Synthesis and magnetic characterizations of manganite-based compostie nanoparticles for biomedical applications. J Appl Phys 2008; **103**: 07P704.

23. **Marques RFC, Jafelicci M, Palva-Santos CO, *et al.*** Nanoparticles synthesis of $La_{1-x}Sr_xMnO_3$ (0.1, 0.2 and 0.3) perovskites. IEEE Trans Magn 2002; **38**: 2892–4.

24. **Grasset F, Mornet S, Demourgues A, et al.** Synthesis, magnetic properties, surface modification and cytotoxicity evaluation of $Y_3Fe_{5-x}Al_xO_{12}$ ($0 \leqslant x \leqslant 2$) garnet submicron particles for biomedical applications. J Magn Magn Mater 2001; **234**: 409–18.

25. **Atsarkin VA, Levkin LV, Posvyanskiy VS, *et al.*** Solution to the bioheat equation for hyperthermia with $La_{1-x}Ag_yMnO_{3-\delta}$ nanoparticles: the effect of temperature autostabilization. Int J Hyperthermia 2009; **25**: 240–7.

26. **Solopan SA, Belous AG, V'yunov OI, Kovalenko LL.** $BaTi_{1-x}Sn_xO_3$ solid solutions: solid-phase and sol-gel syntheses and characterization. Russ J Inorg Chem 2008; **53**: 157–63.

27. **Sakka S.** Handbook of sol-gel science and technology processing, characterization and applications. 2005, Kluwer Academic Publishers.

28. **Belous G, V'yunov O, Pashkova E, *et al.*** Effects of chemical composition and sintering temperature on the structure of $La_{1-x}Sr_xMnO_{3\pm g}$ solid solutions. Inorganic Materials 2003; **39**: 161–70.

29. **Belous AG, Pashkova EV, Vjunov ON, *et al.*** Effect of the emthod of generation on phase transformations, structure and magnetoresistance pattarns of manganites $La_{0.7}Sr_{0.3}MnO_3$. Ukr Chem J 2005; **71**: 17–23 (in Russian).

30. **Pashley RM, Karaman ME.** Applied Colloid and Surface Chemistry. 2004, John Wiley&Sons, Ltd.

31. **Brinker CJ, Scherer GW.** Sol-gel science: the physics and chemistry of sol-gel processing. 1990, San Diego, California: AP, A Division Harcourr Brace&Company.

32. **Kakihana M.** "Sol-gel" preparation of high temperature superconducting oxides. J Sol-Gel Sci Technol 1996; **6**: 7–55.

33. **Volkenstein MV.** Biophysics. 1988, M.: Nauka (in Russian).

34. **Emin D, Holstein T.** Studies of small-polaron motion IV. Adiabatic theory of the Hall effect. Ann Phys 1969; **53**: 439–520.

35. **Snyder GJ, Hiskes R, DiCarolis S, *et al.*** Intrinsic electrical transport and magnetic properties of $La_{0.67}Ca_{0.33}MnO_3$ and $La_{0.67}Sr_{0.33}MnO_3$ MOCVD thin films and bulk material. Phys Rev B 1996; **53**: 14434–44.

36. **Worledge DC, Snyder GJ, Beasley MR, *et al.*** Anneal-tunable Curie temperature and transport of La0.67Ca0.33MnO3. J Appl Phys 1996; **80**: 5158–61.

37. **Loktev VM, Pogorelov YuG.** Peculiar physical properties and the colossal magnetoresistance of manganites. Low Temp Phys 2000; **26**: 171–93.

Copyright © Experimental Oncology, 2011